PHYSICAL REVIEW B **79**, 180509(R) (2009)

Phase diagram of imbalanced fermions in optical lattices

Xiaoling Cui and Yupeng Wang
Beijing National Laboratory for Condensed Matter Physics and Institute of Physics, Chinese Academy of Sciences, Beijing 100190, China

(Received 16 March 2009; revised manuscript received 8 May 2009; published 22 May 2009)

The zero-temperature phase diagrams of imbalanced fermions in three-dimensional optical lattices are investigated to evaluate the validity of the Fermi-Hubbard model. It is found that depending on the filling factor, *s*-wave scattering strength, and lattice potential, the system may fall into the normal (*N*) phase, magnetized superfluid (SF_M), or phase separation of *N* and Bardeen-Cooper-Schrieffer state. By tuning these parameters, the superfluidity could be favorable by enhanced effective couplings or suppressed by the increased band gap. The phase profiles in the presence of a harmonic trap are also investigated under LDA, which show some exotic shell structures compared to those without the optical lattice.

DOI: 10.1103/PhysRevB.79.180509 PACS number(s): 05.30.Fk, 74.20.Fg, 03.75.Ss, 03.75.Hh

In the past few years, great experimental progress has been achieved in studying ultracold Fermi gases with polarization.[1–5] With two unequal mixtures of cold ^{6}Li atoms in a harmonic trap,[1,2] clear evidence of phase separation with an unpolarized superfluid [Bardeen-Cooper-Schrieffer (BCS)] core and a normal (*N*) shell around that has been observed in experiment. Theoretically,[6–13] many other ground-state candidates have been proposed in such systems, including magnetized superfluid (SF_M), phase separation (PS), and Fulde-Ferrell-Larkin-Ovchinnikov (FFLO) state with finite momentum pairing by tuning the interaction parameter at $1/k_F a_s$, the polarization $P=\delta n/n$, or Zeeman field h. Since the optical lattice height V_0 is also tunable, it is very interesting to study its effect on the new phase diagram. For equal mixtures, a second-order quantum phase transition between superfluid (SF) and insulating (IN) phases has been addressed both experimentally at a critical lattice height V_c at resonance[14] and theoretically[15,16] based on the second-order perturbation theory. Besides, there are also works on imbalanced fermions in optical lattices focusing on IN,[17] FFLO,[18] and SF_M (Ref. 19) phases based on an effective Fermi-Hubbard model.

In this work, starting from the exact lattice spectrum, we study the ground-state phase diagram of imbalanced two species Fermi gases trapped in three-dimensional (3D) optical lattices in terms of the total filling factor n, polarization P, *s*-wave scattering length a_s, and lattice potential V_0. Limited by the numerical attainment, the FFLO-type pairing is not considered. The total pairing reciprocal lattice momentums involved in our simulation are up to the six smallest nonzero ones, which turn out to be more and more important as V_0 increases. Sufficient multiple bands have been taken into account to ensure the accuracy especially in the strong coupling regime. We demonstrate that there are two contradictory effects of V_0 on the SF phase, depending on the average filling factor n. One is the enhanced density of states (DOS) inside each band which effectively increases the coupling strength and thus is favorable to SF; the other is the broadened band gap or discontinuity of DOS which is against SF. One key point is that besides tuning a_s through the Feshbach resonance (FR), V_0 can also be tuned and can drive the system from weak to strong coupling regime, provided that the filling factor is properly fixed. Obvious evidence is the emergence of SF_M phase for deep optical lattices at particular filling regimes, even in far BCS side of Feshbach resonance. We also propose that the critical polarization versus total filling factor diagram obtained can be used to evaluate the validity of the usual Fermi-Hubbard model. The phase profile in the presence of an external harmonic trap, which is more relevant to the practical experiment will be studied with local density approximation (LDA) finally. Some exotic structures appear, reflecting the uniqueness of the optical lattices.

In a recent experiment,[14] two hyperfine states of ultracold ^{6}Li atoms, $|F=1/2,\ m_F=1/2\rangle$ ($|\uparrow\rangle$) and $|F=1/2,\ m_F=-1/2\rangle$ ($|\downarrow\rangle$), had been successfully loaded to an optical lattice. The low-energy interactions are characterized by a single *s*-wave scattering length a_s, which can be tuned by FR. Such a system can be well described by the one-channel Hamiltonian,

$$H=\int d\mathbf{r}\sum_{\sigma=\uparrow,\downarrow}\psi_\sigma^\dagger(\mathbf{r})\hat{H}_0(\mathbf{r})\psi_\sigma(\mathbf{r}) + g\int d\mathbf{r}\psi_\uparrow^\dagger(\mathbf{r})\psi_\downarrow^\dagger(\mathbf{r})\psi_\downarrow(\mathbf{r})\psi_\uparrow(\mathbf{r}), \quad (1)$$

where $\hat{H}_0=\Sigma_{i=x,y,z}-\hbar^2\partial_i^2/2M+V_0\sin^2(\pi x_i/a)$; $a=\lambda/2$ is the period of the lattice generated in each direction by two oppositely propagating lasers with wavelength λ; V_0 is the lattice height which is usually measured by the recoil energy $E_R=\frac{\hbar^2\pi^2}{2Ma^2}$; and g is the renormalized contact interaction constant between two species by eliminating the unphysical divergence due to the high-momentum contribution for fermi gases, $\frac{1}{g}=\frac{m}{4\pi\hbar^2 a_s}-\frac{1}{V}\Sigma_q\frac{1}{2\epsilon_q}$.

In the framework of mean-field approach, we expand first each field operator in terms of eigenwave functions of $\hat{H}_0$, $\psi_\sigma(\mathbf{r})=\Sigma_{\mathbf{nk}}\phi_{\mathbf{nk}}(\mathbf{r})\psi_{\mathbf{nk}\sigma}$. The Bloch wave functions $\phi_{\mathbf{nk}}(\mathbf{r})=\frac{1}{\sqrt{V}}\Sigma_{\mathbf{G}}a_{\mathbf{nk}}(\mathbf{G})e^{i(\mathbf{k}+\mathbf{G})\cdot\mathbf{r}}$ and energies $\epsilon_{\mathbf{nk}}$ are obtained from the Schrödinger equation,

$$\sum_{\mathbf{G}'}\left\{\left[\frac{\hbar^2}{2M}(\mathbf{k}+\mathbf{G})^2+\frac{3V_0}{2}\right]\delta_{\mathbf{GG}'} - \frac{V_0}{4}\sum_i\delta_{\mathbf{G}\pm 2\pi/a\mathbf{e}_i,\mathbf{G}'}\right\}a_{\mathbf{nk}}(\mathbf{G}')=\epsilon_{\mathbf{nk}}a_{\mathbf{nk}}(\mathbf{G}), \quad (2)$$

where $\mathbf{n}=\{n_x,n_y,n_z\}=s,p,\ldots$ indicate the band indices, $\mathbf{k}$ lie on the first Brillouin zone (BZ), and $\mathbf{G}=2\pi/a(l_x,l_y,l_z)$ is the reciprocal lattice vector. The solutions satisfy $\Sigma_{\mathbf{G}}a^*_{\mathbf{nk}}(\mathbf{G})a_{\mathbf{n}'\mathbf{k}}(\mathbf{G})=\delta_{\mathbf{nn}'}$ and $a_{\mathbf{n},-\mathbf{k}}(-\mathbf{G})=a^*_{\mathbf{nk}}(\mathbf{G})$. The standard mean-field treatment gives

$$H-\sum_{\sigma}\mu_\sigma N_\sigma=\sum_{\mathbf{nk}\sigma}(\epsilon_{\mathbf{nk}}-\mu_\sigma)\psi^\dagger_{\mathbf{nk}\sigma}\psi_{\mathbf{nk}\sigma}$$
$$-\sum_{\mathbf{mnk}}(\Delta^*_{\mathbf{mnk}}\psi_{\mathbf{m}-\mathbf{k}\downarrow}\psi_{\mathbf{nk}\uparrow}+\text{h.c.})-\frac{V}{g}\sum_{\mathbf{Q}}|\Delta_{\mathbf{Q}}|^2, \tag{3}$$

with

$$\Delta_{\mathbf{Q}}=-\frac{g}{V}\sum_{\mathbf{mnk}}M^{\mathbf{Q}}_{\mathbf{mnk}}\langle\psi_{\mathbf{m}-\mathbf{k}\downarrow}\psi_{\mathbf{nk}\uparrow}\rangle,$$

$$\Delta_{\mathbf{mnk}}=\sum_{\mathbf{Q}}\Delta_{\mathbf{Q}}M^{\mathbf{Q}*}_{\mathbf{mnk}}, \tag{4}$$

and $M^{\mathbf{Q}}_{\mathbf{mnk}}=\Sigma_{\mathbf{G}}a_{\mathbf{m}-\mathbf{k}}(-\mathbf{G})a_{\mathbf{nk}}(\mathbf{G}+\mathbf{Q})$. Since $M^{\mathbf{Q}=0}_{\mathbf{mnk}}=\delta_{\mathbf{mn}}$ and if $m\neq n$ $M^{\mathbf{Q}\neq 0}_{\mathbf{mnk}}$ are quite small, in the following text we only consider pairing within each single band, which means that $\Delta_{\mathbf{mnk}}\approx\Delta_{\mathbf{nk}}\delta_{\mathbf{mn}}$. In such a case, the Hamiltonian can be easily diagonalized, and the thermodynamic potential is calculated at $T=0$ as

$$\frac{\Omega}{V}=\frac{1}{V}\sum_{\mathbf{nk}}\{\Theta(-E_{\mathbf{nk}+})E_{\mathbf{nk}+}+\Theta(-E_{\mathbf{nk}-})E_{\mathbf{nk}-}+\epsilon_{\mathbf{nk}}-\mu$$
$$-\sqrt{(\epsilon_{\mathbf{nk}}-\mu)^2+\Delta^2_{\mathbf{nk}}}\}-\sum_{\mathbf{Q}}\frac{|\Delta_{\mathbf{Q}}|^2}{g}, \tag{5}$$

with $E_{\mathbf{nk}\pm}=\sqrt{(\epsilon_{\mathbf{nk}}-\mu)^2+\Delta^2_{\mathbf{nk}}}\mp h$, where $\mu=(\mu_\uparrow+\mu_\downarrow)/2$ and $h=(\mu_\uparrow-\mu_\downarrow)/2$. From $\partial\Omega/\partial\Delta^*_{\mathbf{Q}}=0$ and $N_\sigma=-\partial\Omega/\partial\mu_\sigma$, we get the gap and density equations as

$$-\frac{\Delta_{\mathbf{Q}}}{g}=\frac{1}{V}\sum_{E_{\mathbf{nk}\pm}>0}\frac{M^{\mathbf{Q}}_{\mathbf{nk}}\Delta_{\mathbf{nk}}}{2\sqrt{(\epsilon_{\mathbf{nk}}-\mu)^2+\Delta^2_{\mathbf{nk}}}},$$

$$n=\frac{1}{N_L}\left(\sum_{\mathbf{nk}}1-\sum_{E_{\mathbf{nk}\pm}>0}\frac{\epsilon_{\mathbf{nk}}-\mu}{\sqrt{(\epsilon_{\mathbf{nk}}-\mu)^2+\Delta^2_{\mathbf{nk}}}}\right), \tag{6}$$

$$\delta n=\frac{1}{N_L}\left(\sum_{E_{\mathbf{nk}+}<0}1-\sum_{E_{\mathbf{nk}-}<0}1\right). \tag{7}$$

Here N_L is the total number of lattice sites; $n=(N_\uparrow+N_\downarrow)/N_L$ and $\delta n=(N_\uparrow-N_\downarrow)/N_L$ are the total filling factor and the difference, respectively. Hereafter we scale all the energies in unit of E_R and the momenta of $2\pi/a$.

To make the numerical simulations attainable but still retain the essence of the problem, besides $\mathbf{Q}=0$ we consider other six nonzero $\mathbf{Q}:(\pm1,0,0),(0,\pm1,0),(0,0,\pm1)$. Due to $M^{\mathbf{Q}}_{\mathbf{nk}}=M^{\pm\mathbf{Q}}_{\mathbf{n}\pm\mathbf{k}}$ and the isotropy of 3D cubic lattices, all six nonzero $\mathbf{Q}$ share the same pairing amplitude Δ_1. Therefore we get two coupled gap equations in terms of Δ_0 and Δ_1. For a realistic numerical simulation, we apply a cutoff momentum $|q_\Lambda|=\frac{3}{2}(1,1,1)$ in the renormalization and correspondingly consider the lowest three bands (s,p,d) in each direction of lattice spectrum. This truncation allows totally $n=54$ atoms per site at most, which is well above the experimental interest as well as ours in this Rapid Communication.

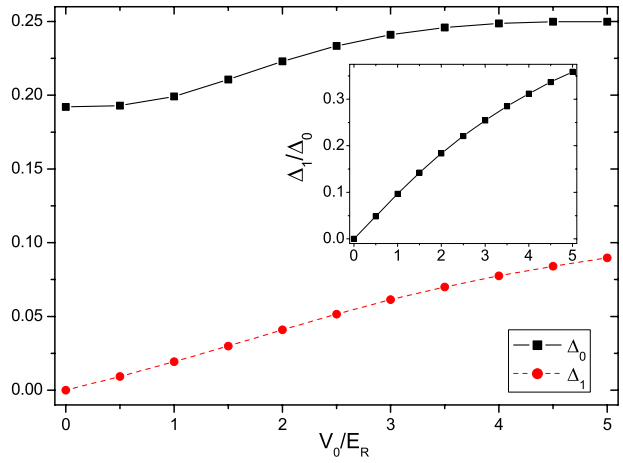

FIG. 1. (Color online) Δ_0, Δ_1, and Δ_1/Δ_0(see inset) vs lattice potentials V_0 for equal mixtures. $a/a_s=-3$. The averaged filling is fixed to be $n=1$.

Before turning to the phase diagram of imbalanced system, first we analyze the necessity of involving nonzero $\mathbf{Q}$ in gap equations for equal mixtures. Figure 1 shows Δ_0, Δ_1, and their ratio as a function of lattice potential V_0 at half filling $n=1$. It is shown that the $\mathbf{Q}\neq0$ pairing becomes more and more important as V_0 increases. This effect can be understood as follows. Taking a very shallow one-dimensional (1D) lattice, for example, nonzero M^Q_{nk} with $|Q|=2,4,6\ldots$ and $1,3,5\ldots$ only exist around kinetic energy-degenerate points $k=0$ and $k=\pm1/2$, respectively, which contribute little to gap equations and therefore produce a negligible Δ_1. In the limit of $V_0=0$, these nonzero M^Q_{nk} exactly cancel with each other in gap equations, and finally only $Q=0$ pairing survives. However as V_0 increases, the eigenvector $a_{nk}(G)$ evolves such that the area of nonzero M^Q_{nk} expands from three discrete points in first BZ to considerable regions around them, leading to an increasing Δ_Q with $Q\neq0$. Since our interest is still within s band, the $|Q|=1$ pairings take a leading role among all nonzero ones, which is verified both numerically and analytically from a perturbation theory for shallow lattices. This is why we just take into account six smallest nonzero $\mathbf{Q}$ in 3D case for not-so-deep lattices. The consideration of nonzero $\mathbf{Q}$ pairing would produce a much stronger superfluidity especially for deep lattices, which can also be seen from the comparison of the previous two works.[20]

The ground-state phase diagram in Fig. 2 is determined as follows. We first compare $\Omega_{\mathrm{BCS}}(\mu,h=E_{\min},\Delta=\{\Delta_0,\Delta_1\})$ with $\Omega_N(\mu,h=E_{\min},\Delta=\{0\})$, with $\Delta_{0/1}$ obtained for unpolarized BCS state and $E_{\min}=\mathrm{Min}_{nk}(\sqrt{(\epsilon_{nk}-\mu)^2+\Delta^2_{nk}})$ as its lowest excitation energy. If $\Omega_{\mathrm{BCS}}>\Omega_N$ then the first-order phase transition point $h_c(<E_{\min})$ is given by

$$\Omega_{\mathrm{BCS}}(\mu,h_c,\Delta=\{\Delta_0,\Delta_1\})=\Omega_N(\mu,h_c,\Delta=\{0\}), \tag{8}$$

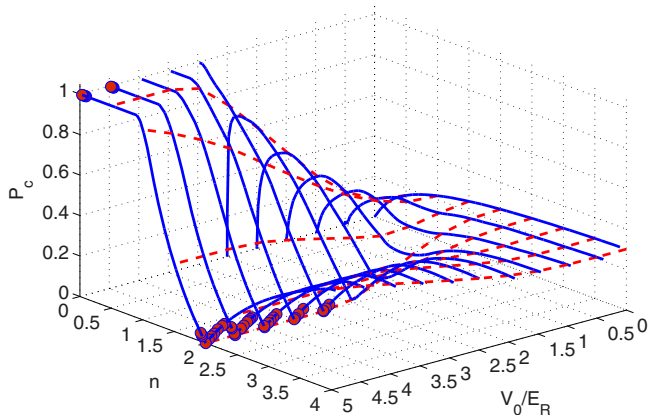

FIG. 2. (Color online) Zero-temperature phase diagram as a function of polarization $P_c=\delta n/n$, total filling factor n, and lattice height V_0. $a/a_s=-3$. The red dashed (blue solid) lines show that P_c evolves with $V_0(n)$ for fixed $n(V_0)$. All the lines above denote the PS-N boundaries, expect for red solid circles separating SF_M and N phase instead.

$$n_N(\mu,h_c)=n. \tag{9}$$

$P_c=\delta n_N(\mu,h_c)/n$ represents a critical point when PS is entirely composed by N phase. Note that in this case the polarized SF or Sarma phase[6] is unstable due to the negative superfluid density.[11] If $\Omega_{\mathrm{BCS}}<\Omega_N$ then there should be a stable SF_M interpolating between BCS and N phase. In free space at the SF_M-N second-order transition point, N denotes a fully polarized normal state with $P_c=1$.[13] Correspondingly in optical lattices, we obtain $P_c=1$ at $n\ll 1$ and $|n-2|/n$ at $n\sim 2$, as shown by solid circles in Fig. 2.

We analyze that P_c-V_0 curves reveal two contradictory effects of increasing V_0 to SF depending on the filling factor n. As shown in Fig. 3, for $n\leq 1$ increasing V_0 will flatten each band and enhance DOS (almost inversely proportional to the band width); while at $n\sim 2$, increasing V_0 produces an entirely opposite effect due to the enlarged band gap. According to the standard BCS theory, the DOS at the Fermi surface dramatically affects the strength of SF, as is also reflected by such contradictory effects. When $V_0=3E_R$, P_c increases to unity at small n but reduces to zero at $n=2$, denoting the IN phase with $n_\uparrow=n_\downarrow=1$. For $n\in(1,2)$, P_c initially drops down and then goes up, indicating the competition between these two effects. Here the lattice enhancement of P_c at $n\leq 1$ is similar to the enhancement of T_c for equal mixtures in weak coupling limit.[21,22]

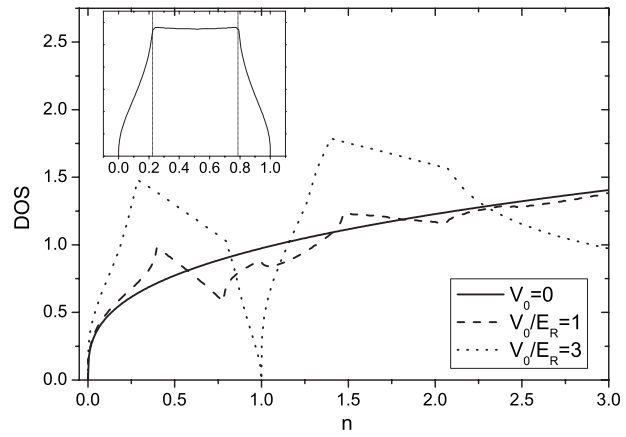

FIG. 3. Density of state DOS at the Fermi surface versus filling factor n for single-spin atoms in 3D free space and in lattices with $V_0/E_R=1$ (no band gap) and $V_0/E_R=3$ (with band gap). Inset is DOS for noninteracting Hubbard model. The dotted lines therein denote two peaks of DOS at $(\mu=t,\ n_p=0.213)$ and $(3t-\mu,1-n_p)$.

Next we turn to P_c-n diagram for fixed V_0. As is well known in free space, a first-order BCS to N phase transition takes place in weak coupling limit at $h_c=\frac{\Delta_0}{\sqrt{2}}$ and $P_c=\frac{3h_c}{2E_F}$, with the gap amplitude $\Delta_0=\frac{8}{e^2}E_F\exp(-\frac{\pi}{2k_F|a_s|})$ and the interaction parameter $\eta=\frac{1}{k_Fa_s}=\frac{a}{a_s}(3\pi^2n)^{-1/3}$. P_c will increase with n all along from weak coupling limit ($\eta\to-\infty$) to the unitary limit ($\eta\to 0$). Within an optical lattice, however, the P_c-n curve would be dramatically modified. In weak coupling limit with small V_0, the curve basically follows as that of DOS in Fig. 3, with a dip at $n_d\sim 2$ and correspondingly a peak at n_p. As V_0 increases, n_p gradually moves to the left and finally vanishes at $n_p=0$, and finally SF_M state emerges at $n\ll 1$ or $n\sim 2$. Different from the SF_M studied by dynamical mean field theory (DMFT) method under tight-binding model,[19] the phase shown here is purely due to the enhanced effective coupling by lattices. In this limit, two fermions are likely to form a molecule, and the BCS equation directly reduces to a Schrodinger equation for a single bound pair.[21,23] It is expected that as V_0 increases, the SF_M phase would extend to a larger or even the whole density region. Actually, the physics at $n\ll 1$ and $n\sim 2$ can be related to each other via particle-hole symmetry. The symmetry is essentially obvious within the background of Fermi-Hubbard model, $\epsilon_{\mathbf{k}}=0.5t\Sigma_i[1-\cos(k_ia)]$. Since (n,μ) and $(2-n,3t-\mu)$ share the same $\{\Delta,h,\delta n,\Omega\}$ and thus the same critical δn_c, the critical polarization $P_c(n)$ for $n\leq 8$ follows as

$$P_c=\begin{cases}1 & n\leq 1\\ \dfrac{|n-2|}{n} & 1<n\leq 5\\ \dfrac{8-n}{n} & 5<n\leq 8\end{cases}. \tag{10}$$

We also compute the phase diagram at other s-wave couplings with fixed V_0 as shown in Fig. 4. Different from Fig. 2, it shows that the increasing a/a_s always enhance SF and improve P_c regardless of filling factors. At sufficiently strong coupling close to unitary, the particle-hole symmetry in each band breaks down since it is energetically favorable for particles in s band to overcome the band gap and form cooper pairs even at $n=2$. In this case the multiband effect should be taken into account. This is why SF_M only turns up at $n\ll 1$ but not at $n\sim 2$ in unitary limit (shown as blue circles in Fig. 4).

We emphasize that the P_c-n diagram in weak coupling limit can be used to evaluate the validity of tight-binding approximation (TBA) usually applied to the lattices. For Hubbard model, the DOS shows two peaks symmetric around half filling (see inset of Fig. 3) due to the van Hove

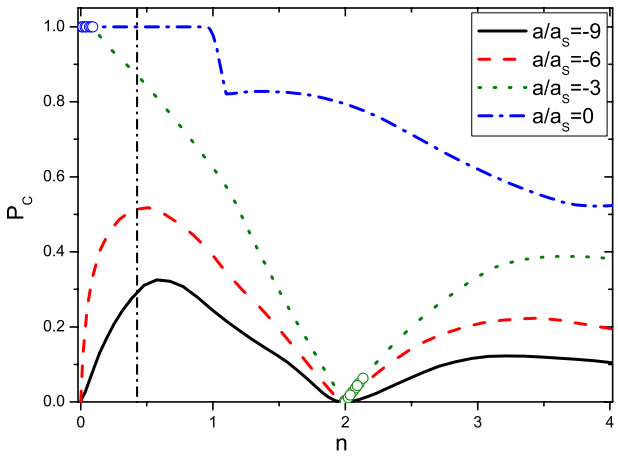

FIG. 4. (Color online) P_c versus n diagram at different couplings. $V_0=3E_R$. All lines denote PS-N boundaries, except that the green and blue circles show SF_M-N boundaries. The black dashed-dot line marks the upper limit of peak position based on Fermi-Hubbard model (see text).

singularity at ($\mu=t$, $n=0.213$) and ($\mu=2t$, $n=0.787$). We also verified numerically that the peak position of P_c at different couplings is never greater than 0.426 for arbitrary interactions $|U|/t$, which is twice as that for the first peak in DOS. This universal property could be used to justify the validity of TBA to realistic lattices. Apparently from Fig. 4 we see that the TBA is not applicable to $V_0=3E_R$ since at really weak coupling ($a/a_s=-9$) the peak position $n_p \simeq 0.6 > 0.426$. The disagreement here indicates the deviation of the two lattice spectrum and, thus, the necessity of adopting exact lattice spectrum for not-so-deep lattices.

Finally, it is also useful to consider the phase profile relevant to realistic experiments with an external harmonic potential $V(\mathbf{r})$. Under LDA, the system is assumed to be locally homogeneous with an averaged chemical potential $\mu(\mathbf{r}) = (\mu_{0\uparrow}+\mu_{0\downarrow})/2 - V(\mathbf{r})$ and a position-independent difference $h=(\mu_{0\uparrow}-\mu_{0\downarrow})/2$. The phase at position $\mathbf{r}$ is determined by the local $[\mu(\mathbf{r}),h]$, which is also self-consistently related to the total particle numbers, the s-wave interaction, and the lattice potential. Here we give several typical phase profiles with the filling factor in trap center larger than 2. For relatively shallow lattices and very weak s-wave interactions, a typical one from the trap center to the edge is: BCS-PN-IN-PN-BCS-PN-FN (PN/FN: partially/fully polarized normal). Starting from this profile, if V_0 increases, PN is very likely to be replaced by SF_M at positions where $n(\mathbf{r}) \sim 2$ or $n(\mathbf{r}) \ll 1$, while IN still survive in a certain region; but if s-wave interaction increases, then IN shrinks gradually, two BCS regimes merge together, and PN gives rise to SF_M, with only three phases left finally: BCS-SF_M-FN. In the latter case, much higher bands with continuous spectrum would be occupied, which makes the situation very similar to free space and the lattice effect is not obvious.

We thank Fei Zhou and An-Chun Ji for beneficial discussions. X.L.C. would like to thank the hospitality of UBC during her stay in Canada, where this work was initially started. This work is in part supported by NSFC under Grant No. 10574150 and 973-Project(China) under Grant No. 2006CB921300.

[1] M. W. Zwierlein, A. Schirotzek, C. H. Schunck, and W. Ketterle, Science **311**, 492 (2006).
[2] G. B. Partridge, W. Li, R. I. Kamar, Y. Liao, and R. G. Hulet, Science **311**, 503 (2006).
[3] M. W. Zwierlein, C. H. Schunck, A. Schirotzek, and W. Ketterle, Nature (London) **442**, 54 (2006).
[4] C. H. Schunck, Y. Shin, A. Schirotzek, M. W. Zwierlein, and W. Ketterle, Science **316**, 867 (2007).
[5] Y. Shin, C. H. Schunck, A. Schirotzek, and W. Ketterle, Nature (London) **451**, 689 (2008).
[6] G. Sarma, J. Phys. Chem. Solids **24**, 1029 (1963).
[7] P. Fulde and R. A. Ferrell, Phys. Rev. **135**, A550 (1964); A. I. Larkin and Y. N. Ovchinnikov, Sov. Phys. JETP **20**, 762 (1965).
[8] P. F. Bedaque, H. Caldas, and G. Rupak, Phys. Rev. Lett. **91**, 247002 (2003).
[9] D. E. Sheehy and L. Radzihovsky, Phys. Rev. Lett. **96**, 060401 (2006).
[10] Z. C. Gu, G. Warner, and F. Zhou, arXiv:cond-mat/0603091 (unpublished).
[11] C. H. Pao, S. T. Wu, and S. K. Yip, Phys. Rev. B **73**, 132506 (2006).
[12] H. Hu and X. J. Liu, Phys. Rev. A. **73**, 051603(R) (2006).
[13] M. M. Parish, F. M. Marchetti, A. Lamacraft, and B. D. Simons, Nat. Phys. **3**, 124 (2007).
[14] J. K. Chin, D. E. Miller, Y. Liu, C. A. Stan, W. Setiawan, C. Sanner, K. Xu, and W. Ketterle, Nature (London) **443**, 961 (2006).
[15] H. Zhai and T. L. Ho, Phys. Rev. Lett. **99**, 100402 (2007).
[16] E. G. Moon, P. Nikolić, and S. Sachdev, Phys. Rev. Lett. **99**, 230403 (2007).
[17] M. Iskin and C. A. R. Sá de Melo, Phys. Rev. Lett. **99**, 080403 (2007).
[18] T. K. Koponen, T. Paananen, J.-P. Martikainen, and P. Torma, Phys. Rev. Lett. **99**, 120403 (2007); T. K. Koponen, T. Paananen, J.-P. Martikainen, M. R. Bakhtiari, and P. Torma, New J. Phys. **10**, 045014 (2008).
[19] T.-L. Dao, M. Ferrero, A. Georges, M. Capone, and O. Parcollet, Phys. Rev. Lett. **101**, 236405 (2008).
[20] Comparing two works on SF-IN transition for equal mixtures at resonance, the critical lattice potential V_c calculated in one (Ref. 16) is almost 1 order of magnitude larger than in the other (Ref. 15) due to the consideration of couplings between different reciprocal lattice vectors.
[21] R. Micnas, J. Ranninger, and S. Robaszkiewicz, Rev. Mod. Phys. **62**, 113 (1990).
[22] W. Hofstetter, J. I. Cirac, P. Zoller, E. Demler, and M. D. Lukin, Phys. Rev. Lett. **89**, 220407 (2002).
[23] P. Nozières and S. Schmitt-Rink, J. Low Temp. Phys. **59**, 195 (1985).